

# Iteration-Perturbation Theory of Covalent Bonding in Crystals\*

## II. Application to Magnesium Hydride $\text{MgH}_2$

Genrich L. Krasko

Institut für Theoretische Physik der Universität Tübingen

Z. Naturforsch. **36a**, 1146–1154 (1981); received September 1, 1981

Using the theory developed in Part I of this work, the calculations of the total energy, equilibrium volume, energy gaps and electronic density distributions are performed for magnesium hydride. The predicted equilibrium atomic volume and energy gaps are close to those observed experimentally. The calculations reveal a strong non-homogeneity in the electron density distribution. The estimated effective charges of the ions of Mg and H are respectively  $+1.90$  and  $-0.65$  which confirms that the bonding in this compound cannot be considered as a purely ionic one.

### 1. Introduction

Hydrogen as a source of energy is considered at present as an option of solving the energy crisis. The problem is actually reduced to hydrogen storage. The best storage "reservoir" is believed to be a crystal lattice, e.g. that of a metal or a compound.

Among various candidates, magnesium as a host atom of a crystal is considered to be rather a prospect, the storage medium itself being magnesium hydride  $\text{MgH}_2$ .

Though the dissociation temperature of  $\text{MgH}_2$  is rather high ( $287^\circ\text{C}$ ) and the kinetics of the hydride reconstruction is complicated, magnesium hydride is used already in practical hydrogen storage for automotive propulsion (see, e.g. [1]). A  $\text{MgH}_2$  reservoir has more than three times the available hydrogen of, e.g., Ti-Fe-H system and promises correspondingly longer range and lighter weight.

The importance of magnesium hydride for hydrogen storage urges its extensive study, both experimental and theoretical. However, very little is known about many basic features of  $\text{MgH}_2$  as a crystal and physical object. At the same time, in order to understand e.g. diffusion processes in the hydride, one has at least to know what kind of a bonding is realized in the crystal, what the energy characteristics of the constituent atoms are, etc.

\* Supported by the Deutsche Forschungsgemeinschaft (DFG) through Grant No. Tu 7/59 (4810/78).

Reprint requests to Prof. Dr. F. Wahl, Institut für Theoretische Physik, Universität Tübingen, Auf der Morgenstelle 14, D-7400 Tübingen.

The crystal structure of magnesium hydride is shown on Figure 1. This is a body-centered tetragonal lattice of the rutile ( $\text{TiO}_2$ ) type (space group  $P4_2/mnm$  ( $D_{4h}^{14}$ )). The lattice is the set of somewhat distorted octahedra of H-atoms inserted into the body-centered tetragonal lattice of Mg-atoms. From the crystallographic point of view the structure is a simple tetragonal lattice with 6 atoms per unit cell: The positions of the atoms are:

$$2\text{Mg}: (000), \left(\frac{1}{2}\frac{1}{2}\frac{1}{2}\right),$$

$$4\text{H}: \pm(x, x, 0), \pm\left(\frac{1}{2} + x, \frac{1}{2} - x, \frac{1}{2}\right);$$

$x$  is the relative shift of H-atoms with respect to Mg-atoms. X-ray study gives for  $\text{MgH}_2$ :

$$a = 4.517 \text{ \AA}, \quad c = 3.021 \text{ \AA},$$

$$x = 0.306, \quad c/a = 0.669$$

(see, e.g. [2]).

$\text{MgH}_2$  is an insulator (see, e.g. [3]), but any experimental results on UV-absorption or photoemission probably have not been reported and the values of energy gaps are unknown.

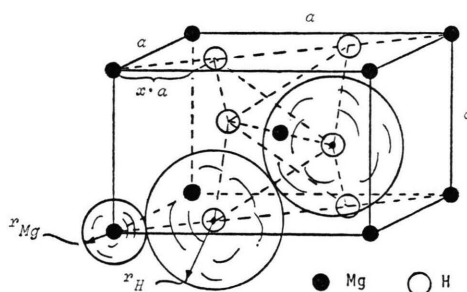


Fig. 1. The unit cell of the rutile-type lattice of  $\text{MgH}_2$ .

0340-4811 / 81 / 1100-1146 \$ 01.00/0. — Please order a reprint rather than making your own copy.



Dieses Werk wurde im Jahr 2013 vom Verlag Zeitschrift für Naturforschung in Zusammenarbeit mit der Max-Planck-Gesellschaft zur Förderung der Wissenschaften e.V. digitalisiert und unter folgender Lizenz veröffentlicht: Creative Commons Namensnennung-Keine Bearbeitung 3.0 Deutschland Lizenz.

Zum 01.01.2015 ist eine Anpassung der Lizenzbedingungen (Entfall der Creative Commons Lizenzbedingung „Keine Bearbeitung“) beabsichtigt, um eine Nachnutzung auch im Rahmen zukünftiger wissenschaftlicher Nutzungsformen zu ermöglichen.

This work has been digitalized and published in 2013 by Verlag Zeitschrift für Naturforschung in cooperation with the Max Planck Society for the Advancement of Science under a Creative Commons Attribution-NoDerivs 3.0 Germany License.

On 01.01.2015 it is planned to change the License Conditions (the removal of the Creative Commons License condition "no derivative works"). This is to allow reuse in the area of future scientific usage.

As for the atomic bonding in  $\text{MgH}_2$  it is believed to be of an intermediate character between a purely ionic one inherent to saline hydrides, like  $\text{LiH}$ , and a covalent one of  $\text{BeH}_2$  [2–4].

The stability of the rutile-type lattice in  $\text{MgH}_2$  is predicted by Pauling ion radii rule ([5], pp. 540–541; [3], p. 387). At the same time calculations of crystal energy within the Born-Mayer model (for the latest results see [6]) show some discrepancies with experimental data being attributed to contributions of covalent effects.

An interesting attempt was performed by Berggren and Lindner [7, 8]. They calculated the lattice energy and equilibrium lattice parameters of  $\text{MgH}_2$  using a nearly-free electron model, i.e. the pseudopotential theory. While the equilibrium lattice parameters for the rutile-type lattice were found to be rather close to those experimentally observed, the lattice itself happened to be relatively less stable than the one of hexagonal type.

With reliable experimental information lacking, it is interesting to perform an “a priori” theoretical analysis of the compound. The microscopic theory developed in Part I of the present work ([9], to be referred to as (I)) enables such an analysis. We shall not have to assume the type of bonding, i.e. the electron density distribution: rather the latter will be obtained as a result of the theory. The only thing we shall have to postulate is the type of lattice, i.e. we shall be considering the  $\text{MgH}_2$  crystal as that of the rutile type. Then the theory is to give an equilibrium (at  $T=0$ ) electron density distribution, atomic volume and crystal lattice parameters:  $c/a$  and  $x$ , as well as the binding energy.

The plan of the paper is as follows: In Sect. 2 the model pseudopotential is chosen and wave-vector sorting is discussed. Jones zone analysis is performed in Section 3. Section 4 considers the computational procedure. The results are presented in Section 5. In Sect. 6 concluding remarks are given.

## 2. Model, Pseudopotential and Wave Vector Sorting

The starting point of our analysis is the rutile-type crystal lattice of  $\text{Mg}^{++}$  and  $\text{H}^+$  ions immersed into electron liquid, consisting of 8 electrons per each unit cell ( $2\text{Mg}^{++}$  and  $4\text{H}^+$  ions; see Figure 1).

The structure factors  $S_{\text{Mg}}(\mathbf{q})$  and  $S_{\text{H}}(\mathbf{q})$  of respectively  $\text{Mg}^{++}$  and  $\text{H}^+$  ions may be readily written:

$$\begin{aligned} S_{\text{Mg}}(\mathbf{q}) &= \frac{1}{N} \sum_{\{\mathbf{R}\}} e^{i\mathbf{q} \cdot \mathbf{R}} (1 + e^{i\mathbf{q} \cdot \mathbf{h}_0}) \\ &= S_0(\mathbf{q}) (1 + e^{i\mathbf{q} \cdot \mathbf{h}_0}), \end{aligned} \quad (1a)$$

$$\begin{aligned} S_{\text{H}}(\mathbf{q}) &= \frac{1}{N} \sum_{\{\mathbf{R}\}} \{e^{i\mathbf{q} \cdot \mathbf{R}} (e^{i\mathbf{q} \cdot \mathbf{h}_1} + e^{-i\mathbf{q} \cdot \mathbf{h}_1}) \\ &\quad + e^{i\mathbf{q} \cdot (\mathbf{R} + \mathbf{h}_0)} (e^{i\mathbf{q} \cdot \mathbf{h}_2} + e^{-i\mathbf{q} \cdot \mathbf{h}_2})\} \\ &= S_0(\mathbf{q}) \cdot 2(\cos \mathbf{q} \cdot \mathbf{h}_1 + e^{i\mathbf{q} \cdot \mathbf{h}_0} \cos \mathbf{q} \cdot \mathbf{h}_2). \end{aligned} \quad (1b)$$

Here

$$\begin{aligned} \mathbf{h}_0 &= a[\tfrac{1}{2}, \tfrac{1}{2}, \tfrac{1}{2}], \quad \mathbf{h}_1 = a[x, x, 0], \\ \mathbf{h}_2 &= a[x, -x, 0]; \end{aligned}$$

$\{\mathbf{R}\}$  is the set of vectors of the simple tetragonal Bravais lattice,  $S_0(\mathbf{q})$  is the structure factor of this lattice:

$$S_0(\mathbf{q}) = \frac{1}{N} \sum_{\{\mathbf{R}\}} e^{i\mathbf{q} \cdot \mathbf{R}} \quad (1c)$$

and  $N$  is the number of unit cells in the cyclic volume  $\Omega = \Omega_0 N$  ( $\Omega_0$  is the volume of the unit cell).

Since the theory (I) is restricted to local electron-ion interaction, the calculations will be performed with a local model pseudopotential. We chose the one suggested by Krasko and Gurskii [10] and successfully used in calculations of atomic properties of some simple metals and their alloys and compounds. The bare pseudopotential formfactor

$$w^0(q) = \frac{4\pi Z}{\Omega_0 q^2} \frac{(2a-1)(qr_c)^2 - 1}{[(qr_c)^2 + 1]^2} \quad (2)$$

depends on two parameters  $a$  and  $r_c$  ( $Z$  is the ion charge). For  $\text{Mg}^{++}$  ion ( $Z=+2$ ) these parameters have been fitted to reproduce the experimentally observed equilibrium atomic volume of pure Mg-metal with hcp-crystal lattice and the pseudopotential formfactor first node  $q_0$  (satisfying  $w^0(q_0)=0$ ). When minimizing the total energy of hcp Mg we used the interpolation formula (I.39c) with  $\alpha=2.5$  for exchange-correlation and the expression of Nozieres-Pines [11] for correlation of homogeneous electron gas. The parameters found in this way are\*

$$a = 2.9330 \quad \text{and} \quad r_c = 0.3990$$

(they slightly differ from those fitted by Fuks et al. [12] with Geldart-Vosco [13] exchange-correlation

\* We use atomic units; energies are calculated in rydbergs.

function). No further fitting of any parameters will be performed.

As for  $H^+$  ions, their potential is purely coulombic:

$$w_H^0(\mathbf{q}) = \frac{4\pi Z_H}{q^2} \quad (Z_H = +1). \quad (3)$$

The plane-wave matrix elements (Fourier-transforms) of the total bare crystal potential are:

$$W^0(\mathbf{q}) = w_{Mg}^0(\mathbf{q})S_{Mg}(\mathbf{q}) + w_H^0(\mathbf{q})S_H(\mathbf{q}). \quad (4)$$

From Eqs. (1a–c) it follows that  $W^0(\mathbf{q})$  vanishes unless  $\mathbf{q} = \{\mathbf{g}\}$ , vectors of the reciprocal lattice corresponding to  $\{\mathbf{R}\}$  — the Bravais simple tetragonal lattice. As one may see from Eqs. (1a–b) and (4),  $W^0(\mathbf{g})$ 's vanish also for some  $\mathbf{q} = \mathbf{g}$  because of symmetry requirements.

According to the method (see Sect. 6 of (I)) one has to sort out the wave vectors  $\{\mathbf{g}\}$ . Having calculated  $W^0(\mathbf{g})$ , Eq. (4) for, e.g., the first 100 reciprocal lattice shells, one may choose the “main” matrix elements, for which the requirements of perturbation theory are obviously violated. Table 1 shows the values  $W^0(\mathbf{g})$  calculated for experimental  $\Omega_0$ ,  $c/a$  and  $x$  for the first 25 reciprocal lattice shells (the third column,  $n$ , is the number of vectors in each shell). Underlined are those values which may

be considered as “main”. Corresponding  $\mathbf{g}$ 's would form the set  $\{\tilde{\mathbf{g}}\}$  (see (I)) of 10 wave vectors.

As a second step the computer program will automatically select all the  $\{\tilde{\mathbf{g}}_0\}$ . Corresponding  $W^0(\mathbf{g})$ 's are small, but “effective” matrix elements,  $\tilde{W}(\mathbf{g})$ , are expected to be appreciably changed in comparison with the screened  $W(\mathbf{g})$ 's (Eq. (I, 11)), because the  $\mathbf{g}$ 's are such that  $\mathbf{g} = \tilde{\mathbf{g}} - \tilde{\mathbf{g}}'$ , i.e. the difference of some two “main” wave vectors.

In practical calculations, however, the choice of the main set,  $\{\tilde{\mathbf{g}}\}$ , does not happen to be as simple as it may seem. The reason is, that after solving selfconsistent equations for  $W(\mathbf{g})$ 's and  $\tilde{W}(\mathbf{g})$ 's, one finds that for some  $\tilde{\mathbf{g}}_0$ 's  $\tilde{W}(\tilde{\mathbf{g}}_0)$  are of the same order as those for the main set, i.e.  $\tilde{W}(\tilde{\mathbf{g}})$ . Such  $\tilde{\mathbf{g}}_0$ 's should obviously be included into  $\{\tilde{\mathbf{g}}\}$ , though corresponding matrix elements,  $W(\tilde{\mathbf{g}}_0)$  are small. After a few trials all the  $\mathbf{g}$ 's which should belong to  $\{\tilde{\mathbf{g}}\}$  may be found. In our calculations for  $MgH_2$  the final sets  $\{\tilde{\mathbf{g}}\}$  and  $\{\tilde{\mathbf{g}}_0\}$  consisted respectively of 31 and 231 wave vectors. Of the wave vectors cited in Table 1 only the last one belongs to  $\{\tilde{\mathbf{g}}_0\}$ ; all the others should be included in  $\{\tilde{\mathbf{g}}\}$ .

For both  $\{\tilde{\mathbf{g}}\}$  and  $\{\tilde{\mathbf{g}}_0\}$  the selfconsistent nonlinear equations for  $W(\mathbf{g})$  and  $\tilde{W}(\mathbf{g})$  were solved. All the other  $\mathbf{g}$ 's were treated within the second-order perturbation theory. The only difference in compar-

Table 1.

$N$ shell	$I J K$	$n$	$g/2k_F$	$W^0(\mathbf{g})$	$W_{fe}(\mathbf{g})$	$W(\mathbf{g})$	$\tilde{W}(\mathbf{g})$	$\tilde{W}(\mathbf{g})$ (equil.)
1	1 1 0	4	0.628	<b>0.0285</b>	0.0188	0.0141	0.0308	0.0315
2	1 0 1	8	0.799	<b>0.0373</b>	0.0316	0.0322	0.0432	0.0419
3	2 0 0	4	0.888	<b>0.0621</b>	0.0569	0.0577	0.0877	0.0864
4	1 1 1	8	0.914	<b>0.0464</b>	0.0432	0.0431	0.0982	0.0982
5	2 1 0	8	0.993	<b>0.0271</b>	0.0262	0.0257	0.0637	0.0638
6	2 2 1	16	1.194	<b>0.0152</b>	0.0151	0.0153	— 0.0103	— 0.0110
7	2 2 0	4	1.256	0.0064	0.0063	0.0065	— 0.0373	— 0.0380
8	0 0 2	2	1.328	0.0034	0.0034	0.0033	0.0585	— 0.0589
9	3 1 0	8	1.404	<b>0.0270</b>	0.0269	0.0269	0.0343	0.0344
10	2 2 1	8	1.421	0.0091	0.0091	0.0091	0.0348	0.0352
11	1 1 2	8	1.469	<b>0.0168</b>	0.0167	0.0167	0.0001	— 0.0002
12	3 0 1	8	1.488	0.0016	0.0016	0.0017	— 0.0508	— 0.0516
13	3 1 1	16	1.553	0.0084	0.0084	0.0084	0.0256	0.0258
14	2 0 2	8	1.597	<b>0.0301</b>	0.0300	0.0300	0.0515	0.0520
15	3 2 0	8	1.602	0.0055	0.0055	0.0048	0.0139	0.0140
16	2 1 2	16	1.658	0.0097	0.0097	0.0095	0.0331	0.0335
17	3 2 1	12	1.733	<b>0.0244</b>	0.0244	0.0242	0.0371	0.0374
18	4 0 0	2	1.776	0.0118	0.0117	0.0118	0.0037	0.0037
19	2 2 2	8	1.828	0.0056	0.0056	0.0057	— 0.0201	— 0.0201
20	4 1 0	8	1.831	0.0121	0.0121	0.0116	0.0411	0.0416
21	3 3 0	8	1.884	0.0031	0.0031	0.0034	— 0.0317	— 0.0322
22	3 1 2	16	1.932	0.0154	0.0153	0.0153	0.0165	0.0167
23	4 1 1	16	1.948	0.0123	0.0123	0.0122	0.0086	0.0087
24	4 2 0	8	1.986	0.0125	0.0125	0.0127	0.0106	0.0107
25	3 3 1	8	1.998	0.0027	0.0027	0.0029	0.0076	0.0076

ison with the traditional approach is that the normalization constant  $C^2$  (Eq. (I, 23)) affects all the calculations.

Until now we do not know anything about the area of occupied electronic states in the crystal. It may well be a Fermi-surface. In this case, the crystal would be a metal or semimetal. Another possibility is a Jones zone (JZ). The latter is possible if the energy gaps on the Bragg planes, restricting an area just necessary and sufficient to accommodate  $Z=8$  electrons, are big enough to overweight competing possibilities of band overlaps.

The following section considers the analysis of the area occupied by the electrons.

### 3. Jones Zone Analysis

In Table 1 the quantities  $g/2k_F$  are also cited. Here  $k_F$  is the free electron Fermi wave vector

$$k_F = \left( \frac{3\pi^2 Z}{\Omega_0} \right)^{1/3}.$$

The area of interest is not a Fermi-sphere, but its total volume must be equal to  $\frac{4}{3}\pi k_F^3$ . It is also clear that the boundary of the area of the occupied states has to be situated somewhere at  $g/k_F \cong 1$ . If the area were a Jones zone, its planes would correspond to  $g/2k_F \cong 1$ . From this point of view three sets of Bragg planes are of interest (see Table 1):  $\{200\}$ ,  $\{111\}$  and  $\{210\}$ .

The Brillouin zone (BZ) of the crystal is a simple tetragonal prism and can accommodate two electrons. Since the total number of electrons per unit cell is 8, 4 BZ's are needed for all the electrons, and that must also be the volume of a JZ.

Let us suppose that a JZ exists in the crystal and is bound by the Bragg planes of  $\{111\}$  and  $\{200\}$ -type. Though we only know  $W^0(\mathbf{g})$ 's, but not the band gaps, one may expect that the latter corresponding to these planes are also the greatest, giving the greatest decrease of energy if the planes are the JZ faces.

Figure 2a shows a BZ prism with the planes of interest. One may see that the  $\{111\}$  and  $\{200\}$  sets of planes really bound the needed area of 4 BZ's. A  $\{111\}$  plane always bisects the BZ, and in order to create a JZ, just 8 truncated BZ-prisms are necessary.

There exist, however, two possibilities: If the tetragonality parameter of the lattice,  $c/a < \sqrt{2}/2$ , then the would-be JZ is bound by the planes of  $\{111\}$

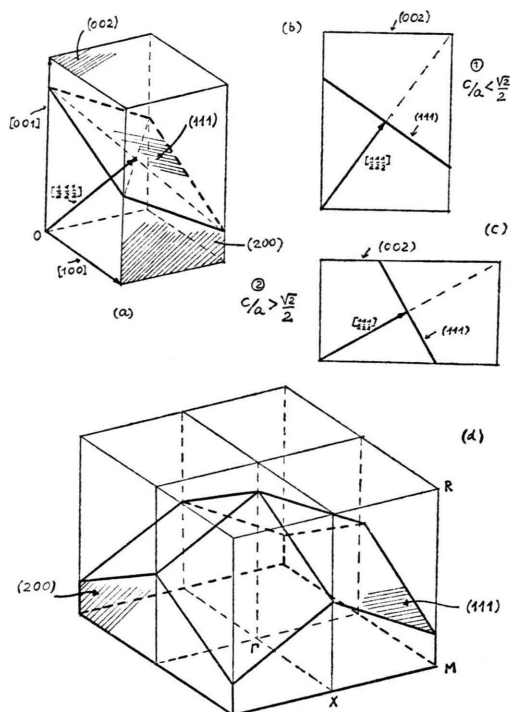


Fig. 2. a) The Brillouin zone of the simple tetragonal Bravais lattice. b) and c) The sections of the Brillouin zone by a  $\{111\}$  Bragg plane in cases  $c/a < \sqrt{2}/2$  and  $c/a > \sqrt{2}/2$  respectively. d) Half of the Jones zone of the magnesium hydride crystal lattice.

and  $\{200\}$ -types (the projection of the planes is shown in Figure 2b). If  $c/a > \sqrt{2}/2$ , then some of the  $\{200\}$  boundary planes are substituted by the  $\{002\}$ -ones (Figure 2c). But the latter is much less favourable, since the  $\{002\}$ -band gap is probably much less than the  $\{200\}$ -ones.

If the  $\{111\}$  and  $\{200\}$ -band gaps are really the greatest, the final conclusion should be, that the magnesium hydride crystal has the JZ bound by these planes (see Figure 2d).

Note that prior to any energy calculations the JZ analysis has enabled us to obtain the information about the tetragonality parameter of the crystal:  $c/a$  has to be less than  $\sqrt{2}/2 = 0.707$ . As was mentioned in the Introduction, the experimentally observed value is equal to 0.669, confirming this condition.

### 4. Computational Procedure

Now that the area of occupied electron states is defined, the procedure of the calculations is as follows.



1. For arbitrary  $\Omega_0$ ,  $c/a (< \sqrt{2}/2)$  and  $x$  the bare pseudopotential matrix elements  $W^0(\mathbf{g})$  are calculated.
2. As a starting point the screened matrix elements  $W(\mathbf{g})$  for all  $\mathbf{g}$ 's are taken to be  $W^0(\mathbf{g})/\epsilon^0(g)$ ,  $\epsilon^0(g)$  being the dielectric function of the free electron gas.
3. The functions  $F(g)$ , Eqs. (I.12), (I.48a–c) are calculated for  $\mathbf{g} \in \{\tilde{\mathbf{g}}\}$  and the set of 27 linear equations, Eq. (I.11) is solved for  $\tilde{W}(\tilde{\mathbf{g}})$ . With the  $\tilde{W}(\tilde{\mathbf{g}})$ 's found,  $\tilde{W}(\mathbf{g})$  are calculated for all  $\mathbf{g} \in \{\tilde{\mathbf{g}}_0\}$  (now (I.11) serve as equalities, the right-hand side sums depending on  $\tilde{W}(\tilde{\mathbf{g}})$ 's only).
4. The functions  $F(g)$  are recalculated for  $\mathbf{g} \in \{\tilde{\mathbf{g}}\}$ ,  $\{\tilde{\mathbf{g}}_0\}$  and calculated for all the other  $\mathbf{g}$ 's (for which  $\tilde{W}(\mathbf{g}) \equiv W(\mathbf{g})$ ).
5. With  $\tilde{W}(\mathbf{g})$ 's for all the  $\mathbf{g}$ 's known, the function  $\Phi(\mathbf{g}, \mathbf{g})$  and the normalization constant,  $C^2$ , is calculated ((I.23), (I.50a–c)).
6. The function  $\Phi(\mathbf{g} - \mathbf{g}', \mathbf{g}')$  and the Fourier-components of the electron density,  $\rho(\mathbf{g})$ , are calculated from (I.25d), (I.51a–c).
7. The screened matrix elements  $W(\mathbf{g})$  are finally evaluated for both  $\mathbf{g} \in \{\tilde{\mathbf{g}}\}$ ,  $\{\tilde{\mathbf{g}}_0\}$  (see (I.26–28)), and all the other  $\mathbf{g}$ 's (I.29).

Now the iteration cycle is completed and the calculations are repeated anew from point 3. The selfconsistency is achieved when the values of the normalization constant,  $C^2$ , in two successive iterations differ less than, e.g. by  $10^{-4}$ . With special measures taken to improve the convergence, the selfconsistency is achieved after five to eight iterations (the matrix element differences are less than  $10^{-5}$ ).

After all the matrix elements are found, the total energy, (I.20a–c), (I.21), is calculated and the pressure

$$P = -\partial E / \partial \Omega_0$$

is found for a given  $\Omega_0$ . Further, the computer program changes  $\Omega_0$  and minimizes the energy (achieving  $p = 0$ ). The corresponding volume  $\Omega_0$  is the equilibrium one.

Likewise the absolute minimum of the total energy with respect to  $c/a$  and  $x$  may be found. In the present paper we report the results for  $c/a$  and  $x$  equal to their experimental values.

## 5. Results

### a) Nonlinear Screening

Table 1 shows also the values of  $W_{\text{fe}}(\mathbf{g})$ , the matrix elements screened by the free electron dielectric function,  $W(\mathbf{g})$ , the genuine screened matrix elements, and  $\tilde{W}(\mathbf{g})$ 's both for experimental and equilibrium atomic volume (the last column)\*. As one can see, the nonlinear screening manifests itself most pronouncely at  $g/2k_F \lesssim 1$ . Most striking is, however, the behaviour of the effective matrix elements,  $\tilde{W}(\mathbf{g})$ , which characterize energy gaps. They are strongly different from  $W(\mathbf{g})$ , and even change sign.

We see that the greatest energy gaps correspond to the JZ faces:  $\mathbf{g} = (111)$  and  $(200)$ . As for the "competing" face,  $(002)$ , its gap, though more than one order of magnitude higher than that, which would correspond to metallic screening, is still some 1.5-times less than the  $(200)$ -gap.

The main energy gaps on the JZ faces  $(111)$  and  $(200)$  for the equilibrium atomic volume (see below) equal:

$$\begin{aligned} \text{gap}(111) &= 2W(111) = 0.3928 \text{ ry} = 5.342 \text{ ev}, \\ \text{gap}(200) &= 2W(200) = 0.3456 \text{ ry} = 4.700 \text{ ev}. \end{aligned}$$

As was mentioned in the Introduction, no experimental data on the electronic band structure of  $\text{MgH}_2$  have yet been reported. However, the recent measurements of UV absorption at Haifa Technion, Israel by Genossar [14] revealed an absorption edge at  $2500 \text{ \AA}$  (5.16 eV) which may be attributed to a band gap. This magnitude is very close to the one obtained theoretically.

### b) Calculation of Electrostatic Energies

The electrostatic energy that the traditional pseudopotential theory usually allows for is that of a positive point ion charge lattice with a uniform negative background. The latter is calculated by the Ewald-Fuchs method (see e.g. [15, 16]). Elec-

\* The symmetry of the rutile-type lattice is lower than that of the simple tetragonal Bravais lattice. As a result in some of the reciprocal shells not all of the  $\mathbf{n}$  wave vectors are equivalent. Within such shells the matrix elements corresponding to half of the wave vectors have opposite sign with respect to that corresponding to another half, though their magnitudes are the same. For convenience all the matrix elements cited in Table 1 are "reduced" to positive sign of  $W^0(\mathbf{g})$  (the matrix elements are cited in hartrees).

trostatic core-core (cc) and core-point (cp) ion interactions are usually neglected.

In the present calculation we took these interactions into account. An a priori reason is that the shortest  $\text{Mg}^{++}\text{-H}^+$  distance in the hydride lattice is rather short ( $\cong 2 \text{ \AA}$ ) and the  $\text{Mg}^{++}$  core- $\text{H}^+$  interaction may, in principle, be important.

The calculations have not approved this claim. Below we cite, however, the results.

The potential that a trial charge feels at a distance  $r$  from an ion may be expressed by a model function

$$v(r) = \frac{Z}{r} + \frac{A^* - Z}{r} e^{-r/r_0} + \frac{B}{r_0} e^{-r/r_c}. \quad (5)$$

Krasko and Shevtsova [17] determined parameters  $A^*$ ,  $B$  and  $r_0$  for ions of 29 elements. Here  $Z$  is the ion charge,  $A^*$  has the meaning of "effective nucleus charge", and  $r_c$  is a characteristic core radius.

For  $\text{Mg}^{++}$  ion the parameters are:

$$A^* = 11.96; \quad B = 2.062; \quad r_c = 0.355$$

(the quantities are in atomic units).

When moving in the field (5), an electron has both ground and excited state levels very close to those experimentally observed for the  $\text{Mg}^{++}$  ion [18].

The additional term in the electrostatic energy,  $E_{\text{es}}^c$ , consists of two contributions:

$$E_{\text{es}}^c = E^{\text{cp}} + E^{\text{cc}} \quad (6)$$

corresponding to  $\text{Mg}^{++}$  core- $\text{H}^+$  point ion and  $\text{Mg}^{++}$  core-core interactions. We included the interactions of up to 6 shells of neighbours. The  $E^{\text{cc}}$  energy happened to be much smaller than  $E^{\text{cp}}$ , as one should have expected. The energy  $E_{\text{es}}^c$  is presented in Table 2 below.

### c) Total and Binding Energies; Equilibrium Atomic Volume

Table 2 shows the results of the calculation of the total energy,  $E_0$ ,  $E_{\text{nc}}$ ,  $E_{\text{xc}}^0$ ,  $\Delta E_{\text{xc}}$ ,  $E_{\text{c}} - E_{\text{el}}$ ,

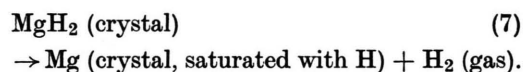
$E_{\text{es}}$ ,  $E_{\text{es}}^c$ , are different contributions (I.20, 21, 42) and (6) to the total energy  $E$  (I.44). (For comparison, the energy that follows from the traditional pseudopotential theory,  $E_{\text{ps}}$ , is also cited.) Note that the "free electron" energy,  $E_0$ , is

$$E_0 = \frac{1}{N} \sum_{jZ} k^2,$$

where the summation is performed over all states within the Jones zone, Fig. 2d, including the spin degeneracy factor 2. The energies in the Table are cited in rydbergs; in the parenthesis are the values of the total energy in kcal.

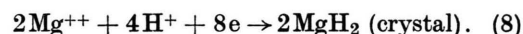
The first line shows the results for the experimentally observed volume of the unit cell,  $\Omega_0 \cong 416.4 \text{ a.u.}$  This volume does not correspond to the energy minimum. The energy minimum is achieved at  $\Omega_0 = 447.5 \text{ a.u.}$  The deviation from the experimental value is:  $\Delta\Omega_0/\Omega_0 = 7.5\%$ .

According to the conditions of experimental determination of the binding energy, the latter is the energy of the chemical reaction:



The usually determined quantity is the enthalpy difference at 298 K,  $\Delta H_{298}$ . For the  $\text{MgH}_2$  crystal to be stable, this quantity must be positive.

On the other hand, the energy  $E$  calculated in our theory is the one of the reaction:



In order to find  $\Delta H_{298}$  if the lattice energy,  $E$ , is known, one should follow a so-called "Born-Haber cycle" (see e.g. [4–6]). The corresponding reactions are cited in Table 3. For simplicity we did not include corrections due to temperature, the latter being of the order of  $RT$  ( $R$  is the gas constant,  $T$  is the absolute temperature), i.e. of the order of a few kcal/mol. Therefore, the quantities cited are  $\Delta H_0$ 's rather than  $\Delta H_{298}$ . We also neglect the

Table 2.

$\Omega_0$ (a. u.)	$k_F$ (a. u.)	$E_0$	$E_{\text{nc}}$	$E_{\text{xc}}^0$	$\Delta E_{\text{xc}}$	$E_{\text{c}} - E_{\text{el}}$	$E_{\text{el}}$	$E_{\text{es}}$	$E_{\text{es}}^c$	$E$	$E_{\text{ps}}$	$\Delta Z$
416.4	0.8286	3.37191	2.04832	-3.87557	0.63845	-2.59988	0.61214	-7.39599	-0.00227	-7.82503 (-2348.9)	-7.29371	3.832
447.5	0.8089	3.21369	1.90585	-3.79449	0.66095	-2.60811	0.61129	-7.22038	-0.00180	-7.84428 (-2357.7)	-7.29044	3.935

Table 3. Born-Haber cycle for  $\text{MgH}_2$  at  $T=0$  K.

Reaction	Evaluation	$\Delta H_0$ kcal/mol
$2\text{H}^+ + 2\text{e} \rightarrow 2\text{H}(\text{gas})$	Ionization potential	— 601.1
$\text{H} + \text{H} \rightarrow \text{H}_2(\text{gas})$	Energy of dissociation	— 99.5
$\text{Mg}^{++} + \text{e} \rightarrow \text{Mg}^+$	2 <sup>nd</sup> ionization potential	— 332.2
$\text{Mg}^+ + \text{e} \rightarrow \text{Mg}(\text{gas})$	1 <sup>st</sup> ionization potential	— 168.9
$\text{Mg}(\text{gas}) \rightarrow \text{Mg}(\text{liq.})$	Heat of vaporization	— 30.1
$\text{Mg}(\text{liq.}) \rightarrow \text{Mg}(\text{cryst.})$	Heat of melting	— 2.1
<hr/>		
$2\text{H}^+ + \text{Mg}^{++} + 4\text{e}$ $\rightarrow \text{Mg}(\text{cryst.}) + \text{H}_2(\text{gas})$		$H_\Sigma = -1233.9$
$\text{Mg}(\text{cryst.}) + \text{H}_2(\text{gas})$ $\rightarrow \text{MgH}_2(\text{cryst.})$	binding energy:	$-H_0$
<hr/>		
$2\text{H}^+ + \text{Mg}^{++} + 4\text{e}$ $\rightarrow \text{MgH}_2(\text{cryst.})$	present calcul.: $E =$ zero point vibrations $E_Z =$	— 1178.9 10.7
<hr/>		
$H_0^f = H_\Sigma - E - E_Z =$		— 65.0 kcal/mol

enthalpy difference between a pure Mg hcp crystal and that saturated with hydrogen, since the limiting concentration of the latter in a primary hcp-solid solution is very low. The zero-point energy,  $E_Z$ , was estimated by Stander and Pacey [6] using their experimental information on IR-absorption spectrum of  $\text{MgH}_2$  \*.

As one can see from Table 3, the binding energy following from the theoretical calculation is negative, while the experimental quantity is positive and equal to

$$17.8 \div 19.9 \text{ kcal/mol}$$

[6, 20, 21]. Such a discrepancy is quite a usual thing for microscopic theories which calculate energies some two orders of magnitude higher than the binding energies of interest. On the other hand, the theory may need further improvement (see the concluding remarks).

#### d) Charge Transfer, Electron Density Distribution and Effective Ion Charges

The last column of Table 2,  $\Delta Z$ , is the charge transfer (I.24). For the crystal in equilibrium,  $\Delta Z = 3.935$  electrons per unit cell are transferred from nearly uniform background and are, in a sense, localized: the number of electrons partic-

ipating in “metallic” screening is  $C^2 Z = Z - \Delta Z$  ( $C^2$  is the normalization constant, see (I.23)).

In order to obtain more detailed information on the electron density distribution, the latter was calculated for three crystallographic planes: (001), (110) and (1 $\bar{1}$ 0). The corresponding two-dimensional plots are shown in Figs. 3a, b and c. For comparison the electronic density distribution in the lattice with the hydrogen atoms removed is also presented (Figure 3d). From Figs. 3a—c one can see that electrons are mainly transferred from the vicinities of  $\text{Mg}^{++}$  ions and the areas just between  $\text{H}^+$  ions in the direction of the z-axis, where the density almost drops to zero. However, not all the electrons are localized near the  $\text{H}^+$  ions. One can see several “electronic bridges”. The most pronounced ones connect  $\text{Mg}^{++}$  ions in the z-direction (see Figure 3b).

It is interesting to estimate the total charges of the areas around the  $\text{Mg}^{++}$  and  $\text{H}^+$  ions. This would give an impression on whether it is worth speaking of the ions of definite charges in the sense of ionic bonding.

Basing on the classical Pauling concepts one may assign definite radii to the ions. If one takes the  $\text{H}^+ - \text{H}^+$  distance along non-horizontal edges of the octahedrons (Fig. 1) as  $2r_{\text{H}}$  — the double radius of a hydrogen ion and the shortest  $\text{Mg}^{++} - \text{H}^+$  distance as  $r_{\text{H}} + r_{\text{Mg}}$ , then (for experimentally observed lattice parameters),

$$r_{\text{H}} = 1.38 \text{ \AA}, \quad r_{\text{Mg}} = 0.57 \text{ \AA};$$

$r_{\text{Mg}}$  is consistent with the traditional ionic radius  $r_{\text{Mg}^{++}} = 0.65 \text{ \AA}$ , while  $r_{\text{H}}$  is almost 1.5 times less than the crystal  $\text{H}^-$  ionic radius  $r_{\text{H}^-} = 2.08 \text{ \AA}$  (see e.g. [5]). Having integrated the electronic density  $\rho(r)$  around the corresponding ions within the spheres of the radii  $r_{\text{H}}$  and  $r_{\text{Mg}}$ , one obtains for the total electronic charges of the spheres:

$$Z_{\text{Mg}} = -0.10, \quad Z_{\text{H}} = -1.65.$$

This means that the Mg-ions have the charges  $+1.90$ , while the charges of H-ions are  $-0.65$ . This is clearly not a picture one would expect for purely ionic bonding. On the other hand, the traditional terms “ionic” and “covalent” do not seem to describe properly the bonding in magnesium hydride. Perhaps a more neutral term, “non-metallic bonding” would suit better.

\* The data on IR absorption spectrum of  $\text{MgH}_2$  were also reported by Mikheeva and Mal'tseva [19].

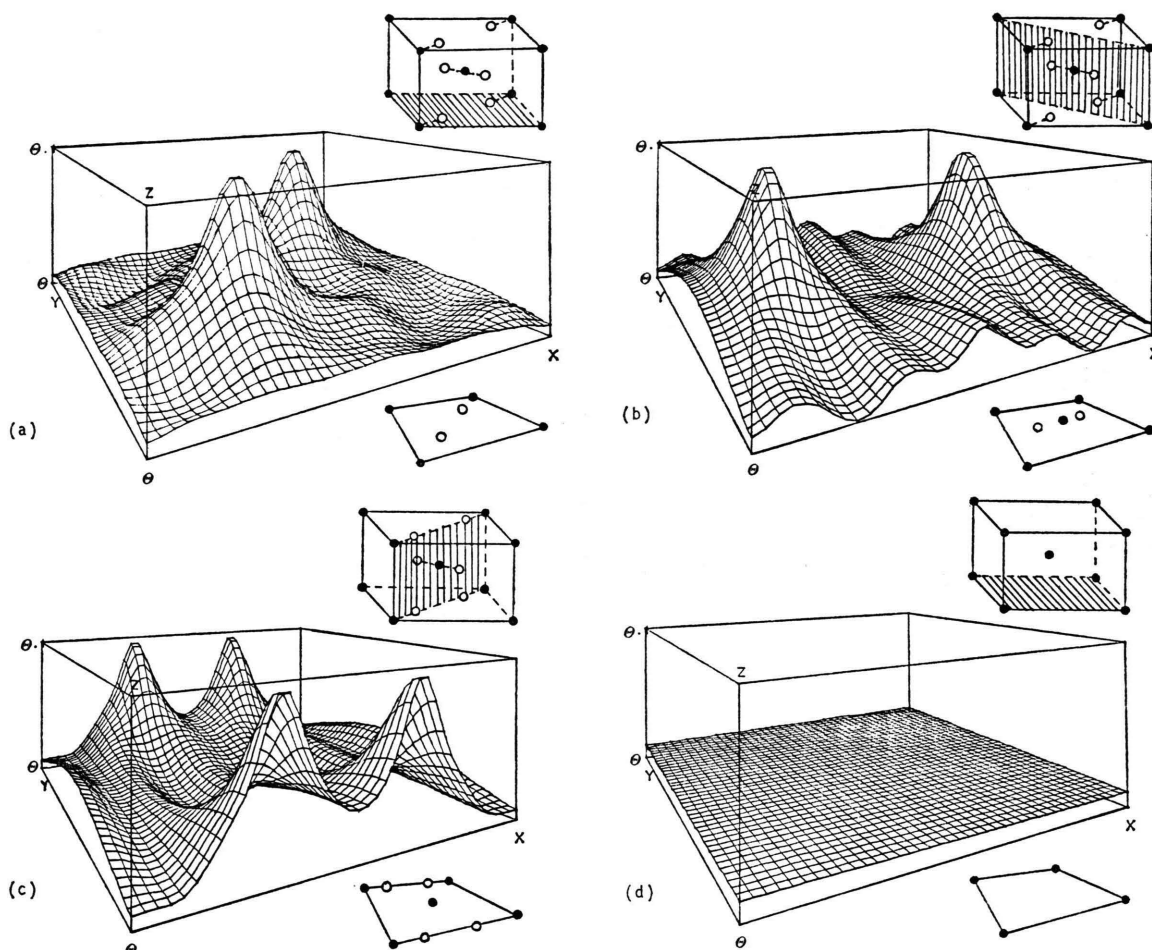


Fig. 3. Electron density distributions in magnesium hydride unit cell: a) Plane (001); b) Plane (110); c) Plane ( $1\bar{1}0$ ); d) Plane (001) with all the hydrogen atoms removed. Black circles are Mg-ions, white circles are H-ions.

## 6. Concluding Remarks

To summarize the results it is worth mentioning once more that the theory developed, in a sense fills the gap between perturbation theory approaches and tight binding methods. Starting from a "metallic" picture, positive  $\text{Mg}^{+2} + \text{H}^+$  ions + free electrons, the theory arrives at an almost purely ionic situation:  $\text{Mg}^{+1.90} + \text{H}^{-0.65}$  + strongly non-homogeneous electronic distribution.

As for the quantitative results, the theory fails to predict the correct binding energy of  $\text{MgH}_2$ , but gives the equilibrium volume and the energy gaps very close to the ones experimentally observed.

Perhaps some improvements of the calculations can be introduced. Unfortunately the TR-440 computer has not enabled us to find the absolute

minimum of the energy with respect to  $c/a$  and  $x$ . Some additional analysis of the exchange-correlation contribution is also necessary. It is not clear as well, whether the results are sensitive to the form of the pseudopotential chosen.

On the other hand, more extensive experimental study of  $\text{MgH}_2$  would give a better basis for comparing the theoretical results with experimental data.

## Acknowledgements

The work was performed through the support of the Deutsche Forschungsgemeinschaft (DFG).

I wish to express my deep gratitude to my colleagues, Prof. F. Wahl and Drs. G. Baumann and B. Schapiro, for hospitality and many fruitful dis-



cussions. I am also grateful to Prof. Jan Genossar from Haifa Technion, Israel, for providing me with the experimental results on UV absorption in

MgH<sub>2</sub> prior to publication, and Dr. Hermann Stoll from the University of Stuttgart for the information on energy levels of the model Mg<sup>++</sup> ion.

- [1] R. Wiswall, in "Hydrogen in Metals II", ed. G. Alefeld, J. Völkl, Springer-Verlag, Berlin 1978, pp. 201—242.
- [2] B. Siegel and G. G. Libowitz, in "Metal Hydrides", ed. W. M. Mueller, J. P. Blackledge, G. G. Libowitz, Academic Press, New York 1968, pp. 545—674.
- [3] T. R. P. Gibb, Jr., in "Progress in Inorganic Chemistry", Vol. III, Interscience Publ., New York 1962, pp. 315—509.
- [4] C. B. Magee, in "Metal Hydrides", ed. W. M. Mueller, J. P. Blackledge, G. G. Libowitz, Academic Press, New York 1968, pp. 165—240.
- [5] L. Pauling, The Nature of the Chemical Bond, Cornell University Press, Ithaca 1960, 3rd edition.
- [6] C. M. Stander and R. A. Pacey, J. Phys. Chem. Solids **39**, 829 (1977).
- [7] K. F. Berggren and P. Lindner, Int. J. Quant. Chem. **48**, 431 (1971).
- [8] P. Lindner and K. F. Berggren, Int. J. Quant. Chem. **VII**, 667 (1973).
- [9] G. L. Krasko, Z. Naturforsch. **36a**, 1129 (1981); Part I.
- [10] G. L. Krasko and Z. A. Gurskii, JETP Letters **9**, 363 (1969).
- [11] P. Nozieres and D. Pines, Phys. Rev. **111**, 442 (1958).
- [12] D. L. Fuks, M. F. Zhorovkov, and V. E. Panin, Phys. Stat. Sol. (b) **70**, 793 (1975).
- [13] D. J. W. Geldart and S. H. Vosko, Can. J. Phys. **48**, 183 (1966).
- [14] J. Genossar, 1980, to be published.
- [15] W. A. Harrison, Pseudopotentials in the Theory of Metals, W. A. Benjamin Inc., New York 1966.
- [16] G. L. Krasko, JETP Letters **13**, 2062 (1971).
- [17] G. L. Krasko and N. A. Shevtsova, Sov. Phys. Dokl. **20**, 565 (1976).
- [18] H. Stoll, 1980, unpublished.
- [19] V. I. Mikheeva and N. N. Mal'tseva, Zh. Strukt. Khim. **4**, 698 (1963).
- [20] J. F. Stampfer, Jr., C. E. Holley, and Suttle, J. Amer. Chem. Soc. **82**, 3504 (1959).
- [21] J. A. Kennelley, J. M. Vorwig, and H. W. Myers, J. Phys. Chem. **64**, 703 (1960).